How to cite: *Angew. Chem. Int. Ed.* **2020**, *59*, 20820–20825
International Edition: doi.org/10.1002/anie.202008784
German Edition: doi.org/10.1002/ange.202008784

Liquid Organic Frameworks | Hot Paper

Liquid Organic Frameworks: A Liquid Crystalline 8-Connected Network with Body-Centered Cubic Symmetry

Changlong Chen[+], Marco Poppe[+], Silvio Poppe, Carsten Tschierske, and Feng Liu**

Abstract: *Liquid state self-assembly is important for the understanding of the complex structures developed in abiogenesis and biogenesis as well as for numerous potential technological applications. Herein we report the first body-centered cubic liquid crystalline phase with 8-connected network topology and open octahedral network structure. It is formed by dynamic soft self-assembly of X-shaped polyphiles with oligo(para-phenylene-ethynylene) cores. The π-conjugated rods with perfluorinated inner benzene rings form networks conjoined by eight-way junctions, which are formed by nano-segregated spheres involving hydrogen-bonded polar end groups, while the branched aliphatic chains at opposite sides of the cores fill the continuum. This novel cubic phase is based on the I-WP minimal surface separating the frameworks of polyaromatic cores from the most disordered chain segments. It can also be considered as a dense sphere packing. Such liquid organic frameworks, representing hybrids of sphere packings and networks could be of interest for organic photonics and other technologies.*

Nanoscale ordered networks are of significant interests as photonic band gap structures, porous materials, transport materials of ions and electrons and numerous other applications.[1] They provide the basis of structural inorganic crystal chemistry,[2] but also play a significant role in soft matter self-assembly. These soft ordered networks are often related to some minimal surfaces with long range periodicity in all three spatial directions (triply periodic minimal surfaces = TPMSs), among which the common phases are bicontinuous cubic phases with gyroid (G), diamond (D) and primitive (P) type periodic surfaces (Figure 1 a–c).[3] These minimal surfaces have a genus of three[4] and separate the space into two equivalent components. Thus, the related structures usually involve two identical or enantiomorphic networks, like the double gyroid (DG, $Ia\bar{3}d$), the double diamond (DD, $Pn\bar{3}m$) and the double "plumber's nightmare" (DP, $Im\bar{3}m$) phases with cubic symmetry, as shown in Figure 1 a–c. Furthermore, the two networks can also be different, like the alternating gyroid (AG, $I4_132$)[5] or only a single network is adopted leading to the single gyroid (SG, $I4_132$),[6] single diamond (SD, $Fd\bar{3}m$)[7] and single "plumber's nightmare" (SP, $Pm\bar{3}m$)[8] phases (see the blue networks in Figure 1 a–c). Double network cubic phases are common in lyotropic and thermotropic liquid crystals, block copolymers and cubosomes. The respective building blocks usually contain two or more different incompatible components (amphiphiles and polyphiles, respectively) so that at least one of them forms the ordered network(s) and the other the continuum.

The 6-connected nets, having the highest valence of their junctions, are related to the P type TPMS (Figure 1 c). The DP

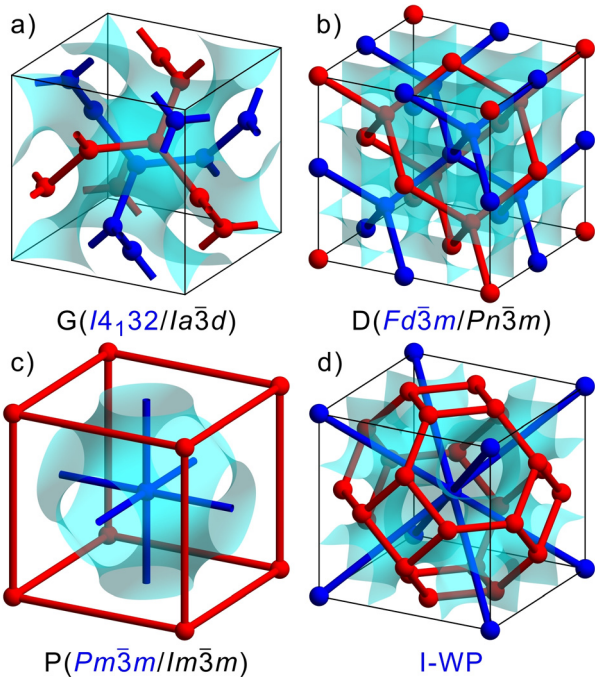

Figure 1. a) G-, b) D-, and c) P-type TPMS in bicontinuous cubic phases with two equivalent networks (shown in blue and red) and the corresponding single network phases (only blue); d) I-WP type TPMS with 8-connected network (blue) and its dual network, corresponding to the edges of the Voronoi polyhedra around the nodes (spheres) and forming truncated octahedra (red, see also Figure S10 in the Supporting Information).

[*] C. Chen,[+] Prof. Dr. F. Liu
State Key Laboratory for Mechanical Behaviour of Materials, Shaanxi International Research Center for Soft Matter, Xi'an Jiaotong University
Xi'an 710049 (P. R. China)
E-mail: feng.liu@xjtu.edu.cn
Dr. M. Poppe,[+] Dr. S. Poppe, Prof. Dr. C. Tschierske
Department of Chemistry, Martin-Luther-University Halle-Wittenberg
Kurt-Mothes Str. 2, 06108 Halle/Saale (Germany)
E-mail: carsten.tschierske@chemie.uni-halle.de
[+] These authors contributed equally to this work.
Supporting information and the ORCID identification number(s) for the author(s) of this article can be found under: https://doi.org/10.1002/anie.202008784.

structure is known for lyotropic systems and was recently found for polymer cubosomes.[9] In contrast, in the thermotropic phases of low molecular weight systems only the non-interpenetrating SP has recently been observed for specifically designed K- and Π-shaped bolapolyphiles.[8] These bolapolyphiles consist of a rigid rod-like core which is terminated by two polar hydrogen bonding glycerol groups with side-on attached flexible lipophilic alkyl/semiperfluorinated chains. This bolaamphiphilic structure favors the network formation by the attractive H-bonding interactions at both ends. The rods form bundles which are interconnected by the polar spheres of the glycerols at the junctions, or the other way around, the rod bundles form a kind of bonds with fixed length between the polar spheres. The volume, shape and distribution of the side chains determine the number of end-to-end arranged bundles between each junction, being either one[8,10] or two,[11] as well as the valence of the network junctions. The 6-connected networks of the SP and DP phases have the highest valence known so far for any self-assembled soft matter system.

Here, we report a novel bicontinuous body-centered cubic LC phase, the first representing an 8-connected network and the first being based on the I-WP surface (Figure 1 d),[12] which separates the space into two different parts, that is, in this case the two networks are intrinsically different. The 8-connected network (blue in Figure 1 d) occupies only one side of the I-WP surface with the flexible side chains fulfilling the space of the 4-connected network on the other side (red, in Figures 1 d and S10). The I-WP surface is also considered as more complex as it owns a genus of four instead of only three of the G, D and P surfaces.[4,13]

This structure is reported here for a X-shaped polyphile **1F** (Table 1) composed of a conjugated oligo(phenyleneethynylene) (OPE) core with two perfluorinated inner benzene rings, bearing two polar glycerol groups at each end and two identical branched aliphatic side-chains at opposite sides.

Compound **1F** was synthesized by a sequence of Sonogashira cross couplings[15] as shown in Scheme 1. Analysis of the

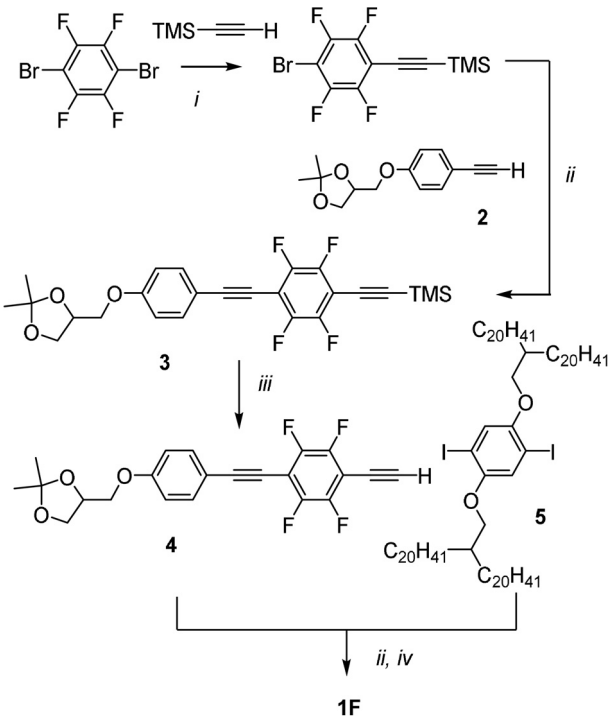

Scheme 1. Synthesis of compound **1F**; Reagents and conditions: *i*) Pd-[PPh_3]$_4$, CuI, Et_3N, reflux; *ii*) Pd[PPh_3]$_2Cl_2$, CuI, Et_3N, reflux; *iii*) K_2CO_3, CH_2Cl_2/MeOH (2/1), 20 °C; *iv*) PPTS, MeOH/THF (1:1), 20 °C.

self-assembly was performed by differential scanning calorimetry (DSC), polarizing optical microscopy (POM) and powder wide angle X-ray scattering (WAXS). Furthermore, synchrotron-based small angle X-ray scattering (SAXS) and grazing incident small angle X-ray scattering (GISAXS) were carried out to elucidate the detailed self-assembled structures formed by this compound. For details of the synthesis, the analytical data and experimental setup, please see SI.

The previously reported analogous non-fluorinated compound **1H** (Table 1)[14] has two LC phases, a square honeycomb with *p4mm* lattice and a lattice parameter $a_{squ} = 4.09$ nm which is in the range of the length of the molecule between the two ends of the two glycerol groups ($L_{mol} = 4.2 \pm 0.2$ nm, see Figure S8). This indicates a square honeycomb in which the rod-like cores form the square cylinders and the side chains fill the resulting prismatic cells. In this square honeycomb the rods are arranged on average perpendicular to the prismatic cell long axes (Figure 2 b) and at the transition to the second low temperature square phase with a smaller $a_{squ} = 3.9$ nm these rods assume a tilt (Figure 2 a). Due to the emerging tilt the prismatic cell volume is adjusted to the reduced space required by the side chains at lower temperature as studied in previous work.[14] The

Table 1: Phases and phase transition temperatures of compounds **1H**[14] and **1F**.

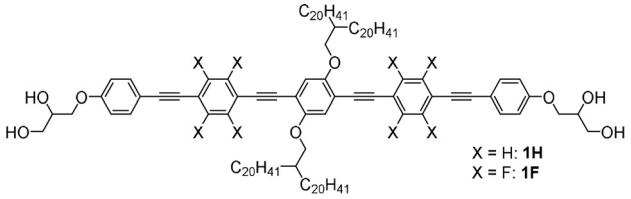

Comp.	X	*T*/°C [Δ*H*/kJ mol^{-1}][a]	*a* [nm] (*T* [°C])
1H	H	H: Cr 47 [21.7] $Col_{squ}{}^{T}$ 89 [1.1] Col_{squ} 130 [9.3] Iso	$a_{squ} = 4.09$ (100)
		C: Iso 128 [10.5] Col_{squ} 88 [1.0] $Col_{squ}{}^{T}$ 31 [30.0] Cr	$a_{squ}{}^{T} = 3.90$ (80)
1F	F	H: Cr 101 [79.2] M 150 [11.8] Col_{squ} 157 [6.6] Cub/$Im\bar{3}m$ 166 [2.0] Iso	$a_{cub} = 5.40$ (160)
		C: Iso 161 [1.9] Cub/$Im\bar{3}m$ 150 [4.4] Col_{squ} 126 [11.2] M 29 [39.6] Cr	$a_{squ} = 4.12$ (150)

[a] Determined by DSC (second heating/cooling, 10 K min^{-1}, peak temperatures); Abbreviations: Cr = crystalline solid; Iso = isotropic liquid state; Col_{squ} = square columnar LC phase with square honeycomb structure and *p4mm* plane group; $Col_{squ}{}^{T} = Col_{squ}$ phase with tilted organization of the rod-like units; Cub/$Im\bar{3}m$ = bicontinuous cubic phase with $Im\bar{3}m$ space group and 8-connected network structure, see explanations in the text for details; M = unknown phase. H = heating, C = cooling, for DSCs see Figure S1e.

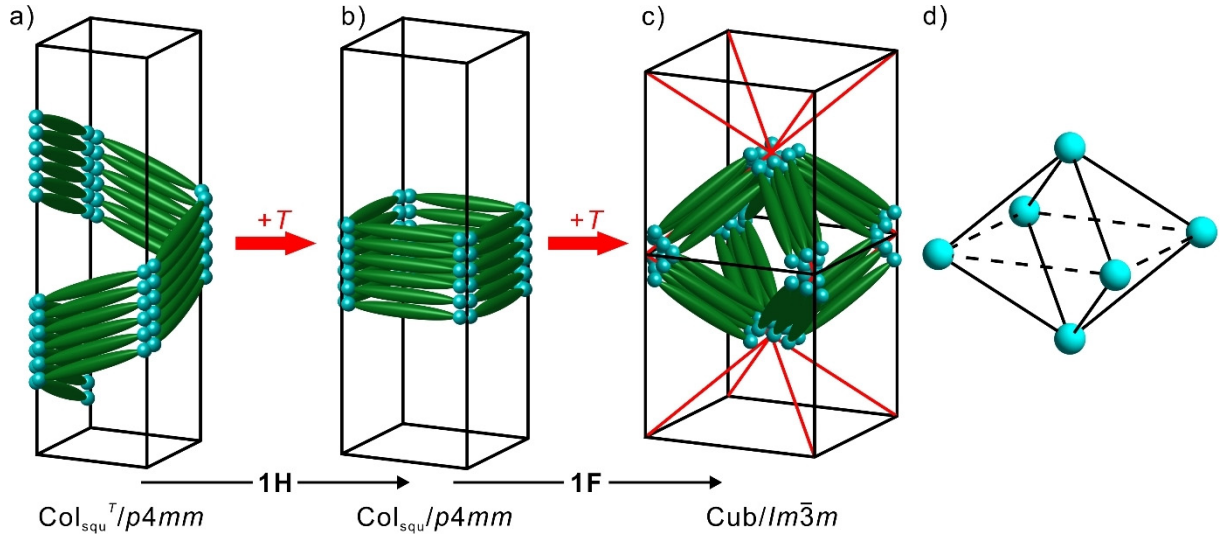

Figure 2. a)–c) Time and space averaged models of the molecular organization in the LC phase structures of compounds **1H** and **1F** and their development depending on temperature; d) shows the "open octahedron" where only the edges of the square plane (dotted lines) are not connected by the OPE cores.

fluorination of the two inner benzene rings of the OPE core leads to a significant stabilization of the LC phases by more than 30 K, despite of the steric effect of perfluorination, usually leading to a strongly reduced LC phase stability (Table 1).[16] This is a first hint on donor-acceptor core-core interactions contributing to the stabilization of the LC phases. However, the phase sequence is also affected by fluorination. The fluorinated compound **1F** shows three enantiotropic liquid crystalline phases: an approximately 10 K broad region of an optically isotropic mesophase at the highest temperature, followed by a short range of a birefringent columnar phase with *p4mm* square lattice and $a_{squ} = 4.12$ nm which is the same as observed for **1H** (Tables 1 and S1, Figures 2b and S2). The transition to the mesophase M at the lowest temperature is anyhow associated with the onset of a tilt of the molecules in the honeycomb walls and in this case leads to a more complex phase which is not yet solved.

The focus here is concentrated on the high-temperature cubic phase of **1F**. The texture under crossed polarizers turns out to be completely dark while the compound showed high viscosity, which is a typical feature of cubic phases (Figure S1a). There exist six sharp peaks in the small angle region of the SAXS pattern whose ratio corresponds to $1{:}2^{1/2}{:}3^{1/2}{:}4^{1/2}{:}5^{1/2}{:}6^{1/2}$ indicating either a cubic $Pm\bar{3}m$ phase or a body-centered cubic $Im\bar{3}m$ phase (Figure 3a). Furthermore, the diffused peak in the wide-angle region supports the liquid crystalline nature, that is, the lack of the individual molecular order (Figure S3b). To confirm the space group of the cubic phase, in situ synchrotron GISAXS experiment was applied to surface aligned samples. The sharp dots are in well accordance with a body-centered cubic phase with $Im\bar{3}m$ symmetry with its closed packed crystal plane (110) parallel to the surface (Figure 3e). Then the powder SAXS diffractogram is indexed with a lattice parameter $a_{cub} = 5.40$ nm. Since the lattice parameter is much larger than the molecular length ($L_{core} = 4.2 \pm 0.2$ nm, Figure S8), it is unlikely to form the bundles along the edges of the cubic lattice as recently reported for the single Plumber's nightmare phase with $Pm\bar{3}m$ lattice.[8] Because a_{cub} is also much smaller than twice the molecular length, a related structure formed by end-to-end arranged molecular pairs[11] can also be excluded. The length of the body diagonal is $L_{diag} = 5.40 \times 3^{1/2} = 9.35$ nm, which is only slightly larger than twice the molecular length. The distance between center and apexes of the unit cell is $L_{diag}/2 = 4.67$ nm. That would be in the range of the length of a hypothetical donor-acceptor pair $L_{d-a} = 4.8 \pm 0.2$ nm having the perfluorinated ring of one compound arranged besides the dialkoxylated middle ring of the adjacent molecule (Figure S8c,d). This longitudinal shift of the molecules in the bundles allows attractive electrostatic interactions between donor and acceptor sites of the cores, and simultaneously it avoids the accumulation of the side chains in the middle (Figure S8). Thus, a bundled model with "longitudinally diffused" molecular bundles along the body diagonals is proposed (Figure 3c).

The electron density map was reconstructed using inversed Fourier Transform (*i*FT) to reveal the self-assembled structure. As shown in Figures 3c and S5a, the high-electron density regions corresponding to the volume fraction of the core parts form the octahedral-type network with 8-connected conjunctions (blue, Figures 1d and S10b), while the dual network with 4-fold junctions shown in red (Figures 1d and S10c) is filled by the low-electron density alkyls (Figure S5b). Furthermore, the simulation of the SAXS results were conducted by the Fourier Transform of the proposed model (see Figure 3d. For detailed simulation, see Section 5 of SI), which compares well with those observed (Figure 3a,b and Table S4).

The length of the side chain in *all-trans* conformation is ≈ 2.8 nm, which is sufficient to easily reach the center of the octahedral cells. The number of molecules in each unit cell is estimated to be ≈ 47, since the number of bundles in a unit

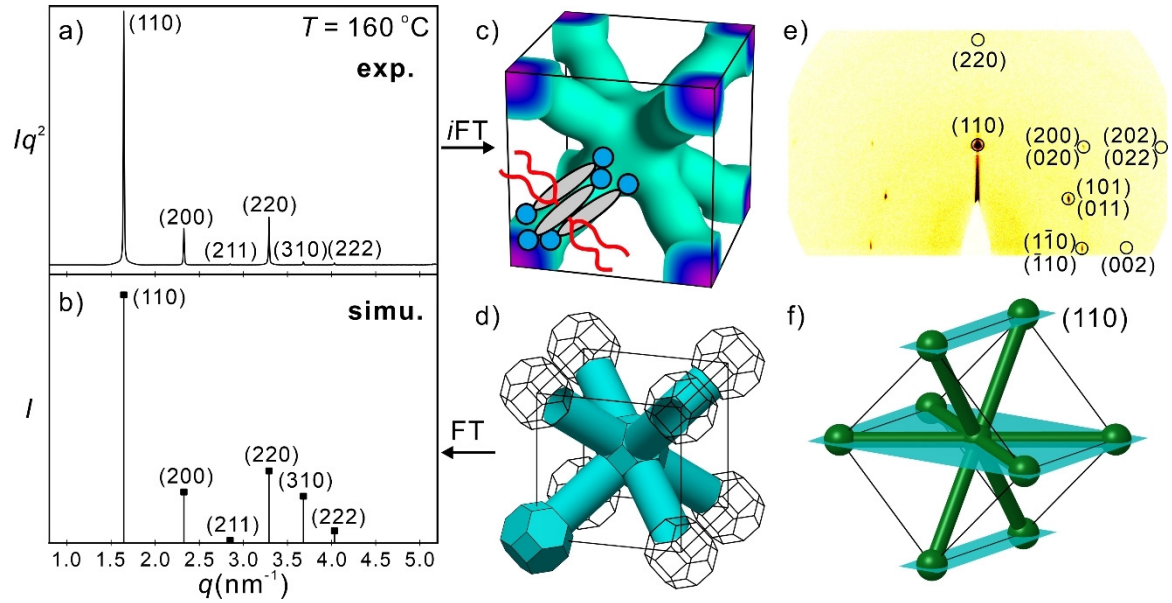

Figure 3. Cub/$Im\bar{3}m$ phase: Experimental (a) and simulated (b) SAXS powder diffractograms at the indicated temperatures; c) Reconstructed ED map from (a), blue-purple = high-density. Inset: schematic molecules. The full ED map is shown in Figure S5b; d) Geometric model used to calculate diffraction intensities shown in (b) and in Table S4, mathematical details are in Section 5 of Supporting Information; e) Experimental GISAXS pattern (sharp spots are from well-oriented domains, with [110] axis perpendicular to the substrate); f) Model of the infinite networks in an $Im\bar{3}m$ unit cell intersected by horizontal (110) planes.

cell is 8, leading to ≈6 molecules in each bundle (Table S3). This is a nearly half of the number of molecules previously reported for the bundles in the cubic phases of T-shaped bolapolyphiles having only one side-chain.[7,11] The reason is obvious, as the X-shaped molecules bear two bulky chains at opposite sides. The molecules cannot easily pack with their non-substituted sides back-to-back. Therefore the cross-sectional shape of the bundles is likely to be elliptically deformed, while being averaged to be circular by time and space averaging (see inset in Figure 4).[17]

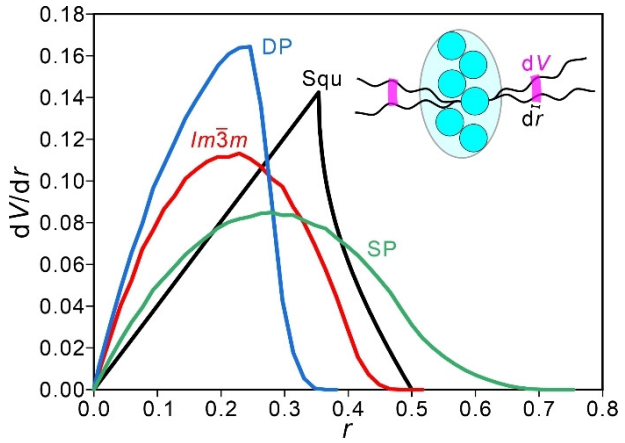

Figure 4. The dV/dr curves of the square columnar phase and different cubic phases, the calculations were performed as explained in Section 7 of the Supporting Information. The inset shows the envelope of aromatic cores viewed along the rod-like cores; the number of molecules is estimated by the ratio of V_{cell}/V_{mol} (Table S3); for a diagram also involving the G and D phases, see Figure S11.

The fluorination of the inner benzene rings plays a dominant role in the formation of such an ordered octahedral-type network, since the molecule without fluorines only shows square columnar phases.[14] As indicated by the WAXS patterns (Figure S3), in the temperature range of the honeycomb phases there are two diffuse scatterings, one at 0.49 nm attributed to the averaged alkyl chain distances and the other one around 0.35 nm is attributed to a face-to-face π-stacking between the cores. This leads to a denser packing of the aromatics in the walls of the honeycomb phase and supports the staggered alternating donor-acceptor packing, supporting a tilted organization of the molecules (Figure S8c,d). Both, the tilt as well as the denser core packing in the walls reduce the space available for the alkyl chains in the square honeycomb cells. This steric frustration increases with rising temperature. Retaining the honeycomb structure by switching to larger pentagonal cells is not possible, because the alkyl chains would not be able to reach the centers of these pentagons without becoming almost completely stretched which is entropically unfavorable (see Section 8 and Figure S12). The alternative option is the disruption of the square honeycomb into a 3D network while the self-assembly in squares is retained. The fused square frames of rod-bundles form the meshes of the developing 3D network (Figure 2b→c). There are three possible structures for networks formed by square or slightly deformed square meshes. The non-interpenetrated SP phase with 6-fold junctions formed by cubic frames, the related interpenetrated DP structure (Figure 1c) and the net with 8-fold junction formed by (open) octahedral frames (Figure 2c). Which of them is chosen depends on the capability of the side chains to fill the space between the nets. The development of the available space for the alkyl chains

depending on the distance from the rod-bundles is shown in Figure 4. Since the mobility of the side chains is higher at elevated temperature, the point of the dV/dr curves[18] dropping to zero should be smaller than in the Col_{squ} phase, where only the DP lattice and 8-connected networks meet this requirement. The 8-connected network structure shows a distribution closer to the square phase than the DP structure. Consequently, the "open octahedral" networks structure (Figure 2c,d) is preferably adopted.

The shift of the rods in the bundles is unavoidably connected with a shift of the glycerols (Figures S7 and S8c,d), thus allowing the formation of larger spheres by supporting a larger valence of the junctions, going beyond only 3–6 as previously found. This increases the impact of the sphere packing on the self-assembly, which is optimized by maximizing the packing density and minimizing the area of the polyhedral Voronoi cells separating the soft spheres.[19] Both favor the body centered $Im\bar{3}m$ lattice over the simple cubic $Pm\bar{3}m$ lattice of the SP phase, whereas the chain volume does not allow the interpenetration of the networks to give the body centered DP structure. Thus, the formation of 8-connected network with open octahedral cells remains the only option. It is suggested that both effects together, the optimization of the space filling between the nets and optimizing the sphere packing, determine the actually chosen cubic phase structure. In the classical bicontinuous cubic phases formed by flexible binary amphiphiles, the TPMS separating the nets determines the valence of the junctions, leading to the DG, DD and DP phases with low connectivity. For the polyphiles, where the nodes of the network form distinct spheres, the optimized packing of these sphere becomes more important and this allows the single network phases to be observed (SD, SP)[7,8] and, in addition, favors higher valences, thus leading to new bicontinuous cubic network phases, representing combinations of networks and spheres.

In conclusion, an 8-connected network with open octahedral cells (Figure 2d) and body-centered cubic lattice, the first one being based on the I-WP minimal surface (Figure 1d), is formed by a star-shaped polyphile with a semiperfluorinated core. The novel structure further develops the complexity of cubic LC phases[20] and provides a transition between the previously separate classes of bicontinuous and micellar cubic phases, that is, between the networks and the sphere packings. The dual nature and modular structure of these LCs composed of rods (bonds) and spheres (nodes) is related to reticular covalent chemistry approaches in the design of solid state materials including COFs and MOFs.[21] This new class of cubic phases can therefore be considered as a showcase for liquid organic frameworks (LOFs)[8] formed in the liquid state by dynamic self-assembly under thermodynamic control.

Acknowledgements

This work is supported by the National Natural Science Foundation of China (No. 21761132033, 21374086) and the Deutsche Forschungsgemeinschaft (392435074). The authors are grateful to Beamline BL16B1 at SSRF (Shanghai Synchrotron Radiation Facility, China) for providing the beamtime. Open access funding enabled and organized by Projekt DEAL.

Conflict of interest

The authors declare no conflict of interest.

Keywords: cubic phases · liquid crystals · liquid organic frameworks · networks · self-assembly

[1] a) A. Angelova, B. Angelov, R. Mutafchieva, S. Lesieur, P. Couvreur, *Acc. Chem. Res.* **2011**, *44*, 147–156; b) Y. Wan, Y. F. Shi, D. Y. Zhao, *Chem. Commun.* **2007**, 897–926; c) T. Kato, M. Yoshio, T. Ichikawa, B. Soberats, H. Ohno, M. Funahashi, *Nat. Rev. Mater.* **2017**, *2*, 20.

[2] A. F. Wells, *Three-dimensional Nets and Polyhedra*, Wiley, New York, **1977**.

[3] L. Han, S. A. Che, *Adv. Mater.* **2018**, *30*, 22.

[4] The genus is the number of "holes" or "handles" a surface has, so that a sphere has genus 0 and a torus has genus 1. The I-WP surface can be considered as a sphere extending handles towards the vertices of a cube (each pair of the 8 vertices form one handle, therefore the genus is 4; For comparsion, the P surface can be regarded as a sphere extending handles towards the face centers, which is 6 leading the genus to 3). The letters WP stand for wrapped package while I indicates the symmetry of body-centered cubic.

[5] a) J. Chatterjee, S. Jain, F. S. Bates, *Macromolecules* **2007**, *40*, 2882–2896; b) C. L. Chen, R. Kieffer, H. Ebert, M. Prehm, R. B. Zhang, X. B. Zeng, F. Liu, G. Ungar, C. Tschierske, *Angew. Chem. Int. Ed.* **2020**, *59*, 2725–2729; *Angew. Chem.* **2020**, *132*, 2747–2751.

[6] V. Saranathan, C. O. Osuji, S. G. J. Mochrie, H. Noh, S. Narayanan, A. Sandy, E. R. Dufresne, R. O. Prum, *Proc. Natl. Acad. Sci. USA* **2010**, *107*, 11676–11681.

[7] X. Zeng, S. Poppe, A. Lehmann, M. Prehm, C. Chen, F. Liu, H. Lu, G. Ungar, C. Tschierske, *Angew. Chem. Int. Ed.* **2019**, *58*, 7375–7379; *Angew. Chem.* **2019**, *131*, 7453–7457.

[8] S. Poppe, X. H. Cheng, C. L. Chen, X. B. Zeng, R. B. Zhang, F. Liu, G. Ungar, C. Tschierske, *J. Am. Chem. Soc.* **2020**, *142*, 3296–3300.

[9] Y. La, C. Park, T. J. Shin, S. H. Joo, S. Kang, K. T. Kim, *Nat. Chem.* **2014**, *6*, 534–541.

[10] S. Poppe, C. Chen, F. Liu, C. Tschierske, *Chem. Commun.* **2018**, *54*, 11196–11199.

[11] a) F. Liu, M. Prehm, X. Zeng, C. Tschierske, G. Ungar, *J. Am. Chem. Soc.* **2014**, *136*, 6846–6849; b) X. Zeng, M. Prehm, G. Ungar, C. Tschierske, F. Liu, *Angew. Chem. Int. Ed.* **2016**, *55*, 8324–8327; *Angew. Chem.* **2016**, *128*, 8464–8467.

[12] A. H. Schoen, *NASA Technical Note TN D-5541* **1970**.

[13] S. Hyde, S. Andersson, K. Larsson, Z. Blum, T. Landh, S. Lidin, B. W. Ninham, *The Language of Shape: The Role of Curvature in Condensed Matter: Physics, Chemistry and Biology*, Elsevier Science B.V., Amsterdam, **1997**.

[14] M. Poppe, C. L. Chen, F. Liu, M. Prehm, S. Poppe, C. Tschierske, *Soft Matter* **2017**, *13*, 4676–4680.

[15] K. Sonogashira, Y. Tohda, N. Hagihara, *Tetrahedron Lett.* **1975**, *16*, 4467–4470.

[16] Y. L. Xu, Y. Q. Hu, Q. Chen, J. X. Wen, *J. Mater. Chem.* **1995**, *5*, 219–221.

[17] a) M. Prehm, F. Liu, X. B. Zeng, G. Ungar, C. Tschierske, *J. Am. Chem. Soc.* **2008**, *130*, 14922–14923; b) M. Prehm, F. Liu, X. B.

Zeng, G. Ungar, C. Tschierske, *J. Am. Chem. Soc.* **2011**, *133*, 4906 – 4916.
[18] X. B. Zeng, G. Ungar, M. Imperor-Clerc, *Nat. Mater.* **2005**, *4*, 562 – 567.
[19] a) P. Ziherl, R. D. Kamien, *J. Phys. Chem. B* **2001**, *105*, 10147 – 10158; b) A. Jayaraman, M. K. Mahanthappa, *Langmuir* **2018**, *34*, 2290 – 2301; c) M. J. Huang, K. Yue, J. Wang, C. H. Hsu, L. G. Wang, S. Z. D. Cheng, *Sci. China Chem.* **2018**, *61*, 33 – 45.
[20] a) S. Kutsumizu, *Isr. J. Chem.* **2012**, *52*, 844 – 853; b) C. Tschierske, *Angew. Chem. Int. Ed.* **2013**, *52*, 8828 – 8878; *Angew. Chem.* **2013**, *125*, 8992 – 9047; c) R. Mezzenga, J. M. Seddon, C. J. Drummond, B. J. Boyd, G. E. Schröder-Turk, L. Sagalowicz, *Adv. Mater.* **2019**, *31*, 1900818.
[21] M. O'Keeffe, O. M. Yaghi, *Chem. Rev.* **2012**, *112*, 675 – 702.

Manuscript received: June 23, 2020
Accepted manuscript online: July 21, 2020
Version of record online: September 7, 2020

